Accepted Manuscript

Effects of cation distribution on microwave dielectric properties of $Mg_{1-x}Zn_xAl_2O_4$ ceramics

Susumu Takahashi, Akinori Kan, Hirotaka Ogawa

PII:	S0254-0584(17)30570-9
DOI:	10.1016/j.matchemphys.2017.07.051
Reference:	MAC 19858
To appear in:	*Materials Chemistry and Physics*
Received Date:	16 January 2017
Revised Date:	31 May 2017
Accepted Date:	13 July 2017

Please cite this article as: Susumu Takahashi, Akinori Kan, Hirotaka Ogawa, Effects of cation distribution on microwave dielectric properties of $Mg_{1-x}Zn_xAl_2O_4$ ceramics, *Materials Chemistry and Physics* (2017), doi: 10.1016/j.matchemphys.2017.07.051

Effects of cation distribution on microwave dielectric properties of $Mg_{1-x}Zn_xAl_2O_4$ ceramics

Susumu Takahashi, Akinori Kan*, and Hirotaka Ogawa

Graduate School of Science and Technology, Meijo University, Nagoya 468-8502, Japan

E-mail:akan@meijo-u.ac.jp

Abstract

The effects of duration of ball-milling on cation distribution of calcined-$MgAl_2O_4$ and -$ZnAl_2O_4$ powders were investigated by ^{27}Al solid-state nuclear magnetic resonance (NMR) measurement; the degree of inversion (λ_C), which corresponds to the fraction of Al^{3+} in tetrahedral site, of the $MgAl_2O_4$ powder increased from 0.33 to 0.42 when the duration of ball-milling varied from 0 to 24 h, though that of the $ZnAl_2O_4$ powders ranged from 0.04 to 0.07. Thus, the preferential occupation of Al^{3+} cation in tetrahedral site was obtained for the calcined-$MgAl_2O_4$ powders prepared by ball-milling for 24 h.

As a result, the $Q \cdot f$ value of the $MgAl_2O_4$ ceramics extremely increased from 85,100 to 187,200 GHz with increasing the duration of ball-milling of the calcined powders, while that of the $ZnAl_2O_4$ ceramics was almost constant with a $Q \cdot f$ value of approximately 100,000 GHz. Moreover, the effects of Zn substitution for Mg on the microwave dielectric properties and cation distribution of the $Mg_{1-x}Zn_xAl_2O_4$ ceramics were also investigated. ^{27}Al NMR measurement revealed that the high λ_0 values, implying the degree of the redistribution of the Al^{3+} cation in the octahedral site during firing, were observed in the composition range of 0-0.75 and the highest $Q \cdot f$ value of 222,600 GHz was obtained for the $Mg_{1-x}Zn_xAl_2O_4$ ceramics at $x = 0.75$. Thus, it is considered that the preferential occupation of Al^{3+} cation at tetrahedral sites of the calcined-powders caused by the ball-milling is effective to enhance the $Q \cdot f$ value of the $Mg_{1-x}Zn_xAl_2O_4$ ceramics.

Keywords: Spinel; Microwave dielectric properties; cation distribution; solid-solutions

1. Introduction

With the rapid development of wireless communication system, the millimeter-wave has been attracted considerable attention for the applications in wireless communication systems such as resonators, filters and substrates, because of high-capacity and high-speed information transfer [1-6]. The low dielectric constant (ε_r) and high quality factor ($Q\cdot f$) are required for the dielectric ceramics to reduce the delay time of electronic signal transmission and to achieve the suppression of signal attenuation. In addition, a near-zero temperature coefficient of resonant frequency (TCf) is also required in these materials. To fulfill such the requirements, the characterizations of microwave dielectric ceramics have been investigated for the various systems [7-11]. The spinel-structured ceramics are known to have a relatively low ε_r and a high $Q\cdot f$ value. Surendran *et al.* [12] reported the microwave dielectric properties of $MgAl_2O_4$ and $ZnAl_2O_4$ ceramics; the ε_r and $Q\cdot f$ values of the $MgAl_2O_4$ ceramic were 8.8 and 68,900 GHz, respectively, while the $ZnAl_2O_4$ ceramic exhibited an ε_r value of 8.5 and a $Q\cdot f$ value of 106,000 GHz, respectively. It is also known that the $MgAl_2O_4$ and $ZnAl_2O_4$ have a normal spinel structure with general formula of $A[B_2]O_4$, where the divalent A^{2+} cation occupy the tetrahedral site, while the octahedral site is occupied by the trivalent B^{3+} cation [13]. However, Šepelák *et al.* reported [14] that the $MgAl_2O_4$ has an intermediate spinel

structure with the general formula of $(Mg_{1-y}Al_y)[Mg_yAl_{2-y}]O_4$, where the degree of inversion, *y*, varied from 0.229 to 0.307. Moreover, Takahashi *et al*. [15] reported that the degree of inversion of $MgAl_2O_4$ ceramics synthesized by molten-salt method was higher than that of the ceramics synthesized by the conventional solid-state reaction method; the higher $Q \cdot f$ value was obtained for the ceramics synthesized by molten-salt method, indicating that the preferential site occupation of Al^{3+} in the tetrahedral site is effective in enhancing the $Q \cdot f$ values of the spinel-structured ceramics. Since the fabrication process and cation distribution of the spinel compounds significantly exerts an influence on the $Q \cdot f$ values, the effects of duration of ball-milling on cation distribution and microwave dielectric properties of $MgAl_2O_4$ and $ZnAl_2O_4$ ceramics were characterized in this study. Moreover, the Zn substitution for Mg was also performed to investigate the relationship between cation distribution and composition dependence of microwave dielectric properties of $Mg_{1-x}Zn_xAl_2O_4$ ceramics.

2. Experimental

The $Mg_{1-x}Zn_xAl_2O_4$ ceramics were prepared by conventional solid state reaction method. MgO (99.99%), ZnO (99.9%) and Al_2O_3 (99.9%) powders were used as the raw materials. The weighted-raw materials were ball-milled in a polyethylene bottle

using yittria-stabilized zirconia balls in ethanol for 24 h, and the mixed slurries were calcined at 1300 °C for 4 h in air. The calcined powders were ground and again ball-milled for 0-24 h, using yittria-stabilized zirconia balls; the calcined $MgAl_2O_4$ (x = 0) and $ZnAl_2O_4$ (x = 1) powders were referred to as MAO*n* and ZAO*n*, respectively, where *n* is duration of ball-milling, ranging from 0 to 24 h. The obtained powders were mixed with the polyvinyl alcohol and uniaxially pressed into pellets with 12 mm in diameter and 7 mm in thickness at 100 MPa. These pellets were fired at the various temperatures ranging from 1500 to 1600 °C for 5 h in air with a heating rate of 5 °C/min. For convenience, the fired $MgAl_2O_4$ and $ZnAl_2O_4$ ceramics are referred to as MA*n* and ZA*n*, respectively. The crystalline phases of samples were identified by X-ray powder diffraction (XRPD), using a Rigaku RINT-2000 diffractometer with a Cu Kα radiation (1.5406 Å). The crystal structure of crystalline phase was refined using the Rietveld analysis [16] software RETAN-FP [17] and the XRPD profiles for the Rietveld analysis were obtained by a step scanning method in the 2θ range of 10 – 120 ° with a step size of 0.03 ° and a counting time of 3.0 sec/step. The cation distribution in the tetrahedral and octahedral sites of the ceramics were investigated from the solid-state ^{27}Al magic angle spinning nuclear magnetic resonance (MAS-NMR) spectra, using JEOL ECA 500 spectrometer with the spinning frequency of 12 kHz. The ε_r and $Q \cdot f$ values of the

ceramics at the room temperature were estimated by Hakki and Coleman method [18, 19], employing a vector network analyzer (Agilent 8720 ES). The temperature coefficient of resonant frequencies (*TCf*) of the samples was determined from the resonant frequencies at 20 and 80 °C. The apparent density of the fired samples was estimated by the Archimedes method. The microstructure of the samples was investigated by a field-emission scanning electron microscopy (FE-SEM; JEOL JSM-6330F). The particle size distribution of the MAO*n* and ZAO*n* powders was measured using the laser diffraction/scattering particle size distribution measuring apparatus (LMS-2000e), taking into account the reported refractive index (n_0) of $MgAl_2O_4$ (n_0 = 1.72) [20] and $ZnAl_2O_4$ (n_0 = 1.80) [21]; the particle size was calculated from the mean area diameter.

3. Results and discussion

3.1. Effects of duration of ball-milling on the cation distribution of $MgAl_2O_4$ and $ZnAl_2O_4$

Figure 1 shows the XRPD profiles of the calcined-MAO*n* and ZAO*n* powders with different duration of ball-milling. All the diffraction peaks were indexed as a cubic spinel structure with a space group of *Fd*3*m* (No. 227), and no evidence of the

diffraction peaks corresponding to the secondary phases was obtained. Based on the XRPD profiles, the full width at half maximum ($FWHM_C$) values of (311) plane of the calcined-MAO*n* and ZAO*n* were summarized in Table 1. The $FWHM_C$ values of both powders depended on the duration of ball-milling, though those of both powders were similar value for the each duration of ball-milling. Moreover, the particle size distributions of the MAO*n* and ZAO*n* powders were measured to clarify the effects of duration of ball-milling on particle size of the powders as shown in Fig. 2. The smaller particle sizes were obtained for both the powders, depending on the duration of ball milling. Based on the particle size distributions, the median size of MAO*n* and ZAO*n* powders are summarized in Table 1. The median sizes decreased from 4.39 to 2.49 μm for MAO*n* powder and from 4.00 to 2.04 μm for ZAO*n* powder, respectively. In addition to the variations in particle sizes, it is considered that the degree of inversion, λ, of the powders depends on the duration of ball-milling because Šepelák *et al.* [14] have reported that the degree of inversion increased from 0.229 to 0.307 when $MgAl_2O_4$ are prepared by the high-energy ball-milling. Therefore, in order to clarify the relationship between the cation distribution and duration of ball milling, ^{27}Al NMR measurements were performed for the MAO*n* and ZAO*n* powders as shown in Fig. 3. The ^{27}Al NMR spectra of both MAO*n* and ZAO*n* powders indicated two signals at approximately 10

ppm and 70 ppm, respectively. According to ^{27}Al NMR spectra of spinel reported by Millard *et al.*[22], the typical two signals at 10 and 70 ppm correspond to a tetrahedrally-coordinated aluminum and an octahedrally-coordinated aluminum, respectively. As for the MAO*n* powders, the intensity of signal at 70 ppm of MAO24h powder was higher than those of MAO0h and MAO4h powders, while the intensity of signals at 10 ppm was slightly low in comparison with those of MAO0h and MAO4h powders. In contrast, the intensities of signals of ZAO*n* powders were independent of the duration of ball-milling. These results imply that the duration of ball-milling only affected exerts an influence on the cation distribution of Al^{3+} in the $MgAl_2O_4$ lattice. Thus, it is considered that $MgAl_2O_4$ has an intermediate spinel structure which corresponds to $(Mg_{1-\lambda}Al_{\lambda})[Mg_{\lambda}Al_{2-\lambda}]O_4$ with the various λ values, whereas $ZnAl_2O_4$ has an intermediate one with lower λ values which close to a normal spinel structure. Based on these NMR spectra data, the degree of inversion (λ_C) values of MAO*n* and ZAO*n* powders were estimated using the following equation:

$$\frac{I(AlO_4)}{I(AlO_6)} = \frac{\lambda_C}{2-\lambda_C} \qquad (1)$$

where, $I(AlO_4)$ and $I(AlO_6)$ indicate the peak intensities of signals at the tetrahedrally-coordinated aluminum at 70 ppm and the octahedrally-coordinated aluminum at 10 ppm, respectively [23]. The λ_C values of MAO*n* and ZAO*n* are summarized in Table 1.

The λ_C values of MAO*n* powders were higher than those of ZAO*n* powders; these λ_C values of MAO*n* increased from 0.33 to 0.42 with increasing the duration of ball-milling, while ZAO*n* powders slightly increased from 0.04 to 0.06. From the estimation of the λ_C values, it is also found that Mg^{2+} cation can occupy both the tetrahedral and octahedral site in MAO*n*, though most of all Zn^{2+} cations occupy the tetrahedral site in ZAO*n*. Since the remarkable differences in the λ_C value between MAO*n* and ZAO*n* powders are observed in this study, it is expected that the duration of ball-milling significantly exerts an influence on the microwave dielectric properties. Thus, the MA*n* and ZA*n* ceramics were prepared by using the MAO*n* and ZAO*n* powders.

The crystal structure parameters of the MA*n* and ZA*n* ceramics were summarized in Table 2; the effect of the duration of ball milling on the crystal structure parameters of both ceramics was not observed. ^{27}Al NMR spectra of both MA*n* and ZA*n* ceramics fired at 1600 °C for 5 h were measured and the λ_F values of the fired ceramics were also calculated as listed in Table 1. The λ_F values of MA*n* ceramics increased from 0.27 to 0.29 with increasing the duration of ball-milling of MAO*n* powders, while those of ZA*n* ceramics was almost constant (λ_F = 0.03). Moreover, the degree of redistribution of Al^{3+} cation in octahedral site during firing (λ_0) is calculated by the following equation:

$$\lambda_0 = \lambda_C - \lambda_F \quad (2).$$

The λ_0 values of MA*n* and ZA*n* are listed in Table 1. The λ_0 values of MA*n* were higher than those of ZA*n* and the λ_0 values increased from 0.06 to 0.13 for the MA*n* and 0.01 to 0.04 for the ZA*n*, respectively, depending on the duration of ball-milling of the calcined powders. In the $MgAl_2O_4$ synthesized by molten-salt synthesis, it is found that the λ_0 value relate with the crystallinity, grain growth and densification of the ceramics [24]. Thus, it is considered that the higher λ_0 values of MA*n*, i.e., redistribution of Mg^{2+} and Al^{3+} cations in the lattice during firing, lead to the enhancement of the crystallinity, grain growth and densification of MA*n*. The surface microstructures of MA*n* and ZA*n* fired at 1600 °C for 5 h are shown in Fig. 4; the morphological changes in MA*n* and ZA*n* are observed as expected from the difference in λ_0 values. The average grain size is calculated using a linear intercept method by counting the adjacent grains in the SEM images. The average grain sizes of MA0h and ZA0h are 1.6 and 1.8 μm, respectively, whereas those of MA24h and ZA24h are 4.1 and 2.2 μm, respectively; the densed microstructure was observed for MA24h. The morphological changes in MA*n* and ZA*n* are attributed to the difference in the λ_0 values between MA*n* and ZA*n*. The relative densities of MA*n* and ZA*n* ceramics are summarized in Table 3. The increase in relative density was obtained for MA*n* ceramics; the relative densities of MA*n* ceramics increased from 94.8 to 96.6% with increasing the duration of ball-milling, while those

of the ZA*n* ceramics slightly increased from 95.2 to 95.8%. In addition to the variation in the relative density, the differences in the $FWHM_F$ values of the MA*n* and ZA*n* were also observed as listed in Table 1; the $FWHM_F$ value of the MA24h ($FWHM_F$ = 0.138) was lower than that of ZA24h ($FWHM_F$ = 0.152), though those of both MA*n* and ZA*n* were similar values when the duration of ball-milling ranged from 0 to 4 h. It is considered that the higher redistribution of constituent cation during firing also lead to the higher crystallinity of the ceramics. The microwave dielectric properties of the MA*n* and ZA*n* ceramics are listed in Table 3. The ε_r values the MA*n* increased from 7.8 to 7.9 with increasing the duration of ball-milling of MAO*n* powder, though that of the ZA*n* was almost constant (ε_r = 8.5) because of the increase in the relative density of the MA*n*. Moreover, the remarkable differences in $Q \cdot f$ value were observed for the MA ceramics; the $Q \cdot f$ values of the MA*n* ceramics remarkably increased from 87,300 to 187,200 GHz when the duration of ball-milling for the MAO*n* powders varied from 4 to 10 h, though those of the ZA*n* ceramics were independent of duration of ball-milling. Thus, it is considered that the significant increase in the $Q \cdot f$ value of the MA*n* ceramics is related with the preferential occupation of Al^{3+} cation at tetrahedral site of calcined-MAO*n* powders which lead to higher crystallinity of MA*n* ceramic.

3.2. Effects of Zn substitution for Mg on cation distribution and microwave

dielectric properties of the $Mg_{1-x}Zn_xAl_2O_4$ ceramics

The XRPD profiles of the $Mg_{1-x}Zn_xAl_2O_4$ ceramics fired at 1600 °C for 5 h are shown in Fig. 5. For all the compositions, the diffraction peaks corresponded to the cubic structure with space group of *Fd*3*m* and shifted to lower 2θ as shown in Fig. 5 (b), depending on the composition *x*. Such peak shift is considered to be related to a difference in the ionic radii between Mg^{2+} and Zn^{2+} cations [25]. Based on these XRPD profiles, therefore, the crystal structure parameters of $Mg_{1-x}Zn_xAl_2O_4$ ceramics were refined by Rietveld analysis and were listed in Table 4. The lattice parameter of the ceramics increased from 8.0677(9) Å to 8.0793(4) Å with increasing the composition *x* because the ionic radius of Mg^{2+} (0.57 Å) cation was smaller than that of Zn^{2+} cations (0.60 Å) [25]. The $FWHM_C$ and $FWHM_F$ values of (311) plane of the $Mg_{1-x}Zn_xAl_2O_4$ ceramics are summarized in Table 5. For the all compositions, the $FWHM_C$ value of the calcined $Mg_{1-x}Zn_xAl_2O_4$ powders was a similar value (0.26°). Since the $FWHM_F$ value of the fired $Mg_{1-x}Zn_xAl_2O_4$ ceramics in the composition range of 0-0.75 (0.13°) was lower than that of the ceramic at x = 1 (0.15°), the high crystalline phase was obtained in the composition range of 0-0.75; the partial Zn substitution for Mg was effective in improving the crystallinity of spinel compounds. Figure 6 shows the ^{27}Al NMR spectra of the $Mg_{1-x}Zn_xAl_2O_4$ ceramics. The spectra slightly shifted to low-field with increasing

the composition *x* because of the second-order quadrupolar order shifts, and such the difference in the chemical shift between the $MgAl_2O_4$ and $ZnAl_2O_4$ was also reported by Pellerin *et al*. [26]. As for the calcined $Mg_{1-x}Zn_xAl_2O_4$, the intensity of ^{27}Al NMR spectra at 70 ppm decreased with increasing the composition *x*, suggesting that the Al^{3+} cation preferentially occupies the tetrahedral site by the Zn substitution for Mg. Moreover, the intensities of the spectra at 70 ppm for the fired $Mg_{1-x}Zn_xAl_2O_4$ ceramics are weak in comparison with those of the calcined ceramics, implying that the redistribution of Al^{3+} cation in the octahedral site is enhanced during firing. Thus, based on these NMR data, λ_C and λ_F values of $Mg_{1-x}Zn_xAl_2O_4$ were calculated as listed in Table 5. The λ_C and λ_F values of the $Mg_{1-x}Zn_xAl_2O_4$ decreased by Zn substitution for Mg; the Zn substitution for Mg of $Mg_{1-x}Zn_xAl_2O_4$ ceramics lead to the preferential occupation of Al^{3+} cation in the octahedral site. Moreover, the λ_0 values increased from 0.13 to 0.17 in the composition range of 0-0.75, while the λ_0 value at $x = 1$ was 0.04. Therefore, the variation in λ_0 value may relate with the crystallinity of the $Mg_{1-x}Zn_xAl_2O_4$ ceramics which leads to the enhancement of $Q \cdot f$ values. The variations in relative densities and ε_r values of the $Mg_{1-x}Zn_xAl_2O_4$ ceramics fired at 1600 °C are shown in Fig. 7. The relative density of the $Mg_{1-x}Zn_xAl_2O_4$ ceramics was approximately 96% in the composition range of 0-0.75, while that of the ceramics at $x = 1$ was 95%. It

is considered that the high relative density of the ceramics in the composition range of 0-0.75 is related with the high λ_0 value of the ceramics, which exerts an influence on the grain growth. As for the ε_r value of the $Mg_{1-x}Zn_xAl_2O_4$ ceramics, the ε_r value of the ceramics increased from 7.9 to 8.5 with increasing the *x* value because an ionic polarizability of Zn cations (2.04 $Å^3$) is higher than that of Mg cation (1.32 $Å^3$) [27]. Zheng *et al*. [28] also reported that the ε_r value of the densed $Mg_{1-x}Zn_xAl_2O_4$ ceramics gradually increased from 7.9 to 8.6 by the Zn substitution for Mg; the variation in the ε_r value of the $Mg_{1-x}Zn_xAl_2O_4$ ceramics in present study was similar to that reported by Zheng *et al*. Figure 8 shows $Q{\cdot}f$ and *TCf* values of $Mg_{1-x}Zn_xAl_2O_4$ ceramics fired at 1600 °C for 5 h. The $Q{\cdot}f$ values of the $Mg_{1-x}Zn_xAl_2O_4$ ceramics increased from 187,200 to 222,600 GHz with increasing the *x* value in the composition range of 0-0.75, and the $Q{\cdot}f$ values of the ceramics extremely decreased to 108,500 GHz by the further increase in composition up to $x = 1$. It is implied that the high $Q{\cdot}f$ values in the composition range of 0-0.75 are related to the high λ_0 value of the $Mg_{1-x}Zn_xAl_2O_4$, which leads to the higher crystallinity of the ceramics. Thus, the preferential occupation of Al^{3+} cation in tetrahedral sites of the calcined-$Mg_{1-x}Zn_xAl_2O_4$ powders caused by the ball-milling leads to the increase in the $Q{\cdot}f$ values of the ceramics. The difference in *TCf* value of $Mg_{1-x}Zn_xAl_2O_4$ ceramics was not recognized; the value of the ceramics was approximately -

60 ppm/°C. Therefore, the effect of the Zn substitution for Mg on the *TCf* value of the $Mg_{1-x}Zn_xAl_2O_4$ ceramics is considered to be small.

4. Conclusions

^{27}Al solid-state nuclear magnetic resonance (NMR) measurement suggested that the λ_C value, which corresponds to the fraction of Al^{3+} in tetrahedral site, of the $MgAl_2O_4$ powder increased from 0.33 to 0.42, depending on the duration of ball-milling, while that of the $ZnAl_2O_4$ powders slightly increased from 0.04 to 0.07; the preferential occupation of Al^{3+} cation at tetrahedral sites of $MgAl_2O_4$ lattice were caused by the ball-milling with longer duration. As a result, the $Q{\cdot}f$ value of the $MgAl_2O_4$ ceramics extremely increased from 85,100 to 187,200 GHz with increasing the duration of ball-milling, though that of the $ZnAl_2O_4$ ceramics was a slight increase from 93,300 to 108,500 GHz. Moreover, the higher $Q{\cdot}f$ values of $MgAl_2O_4$ ceramics were obtained in the composition range of 0.25-0.75 by the Zn substitution for Mg, leading the increase in the λ_0 value which corresponds to the degree of the redistribution of the Al^{3+} cation in the octahedral site during firing; the ceramics at $x = 0.75$ exhibited the highest $Q{\cdot}f$ value of 222,600 GHz. It is found that the preferential occupation of Al cations at tetrahedral sites of the calcined-powders caused by the ball-milling is considered to be effective in

improving the $Q \cdot f$ value of the spinel ceramics.

Acknowledgment

This work was supported by Grant-in-Aid for JSPS Research Fellow Grant Number JP16J11394.

References

[1] Y.-C. Chen and H.-M. You, Mater. Chem. Phys. 154 (2015) 94.

[2] Q. Ma, S. Wu and Y. Fan, Ceram. Int. 40 (2014) 1073.

[3] T. Tsunooka, H. Sugiyama, K. Kakimoto, H. Osato and H. Ogawa, J. Ceram. Soc. Jpn. 112 (2004) S1637.

[4] I. S. Ghosh, A. Hilgers, T.Schlenker and R. Porath, J. Eur. Ceram. Soc. 21 (2001) 2621.

[5] J. Zhang, R. Zuo, Y. Wang and S. Qi, Mater. Letters. 164 (2016) 353.

[6] Li. He, S. –B. Mi, X. Jin, H. Zhang, D. Zhou, F. Xiang, H. Yang and H. Wang, J. Am. Ceram. Soc. 98 (2015) 2122.

[7] M. Ando, H. Ohsato, I. Kagomiya, and T. Tsunooka, Jpn. J. Appl. Phys. 47 (2008) 7729.

[8] Y. Guo, H. Ohsato and K. Kakimoto, J. Eur. Ceram. Soc. 26 (2006) 1827.

[9] S. Wu, C. Jiang, Y. Mei and W. Tu, J. Am. Ceram. Soc. 96 (2012) 37.

[10] H. Ogawa, A. Kan, S. Ishihara and Y. Higashida, J. Eur. Ceram. Soc. 23 (2003) 2485.

[11] J. C. Kim, M. –H. Kim, J. =B. Lim and S. Nahm, J. Am. Ceram. Soc. 90 (2007) 641.

[12] K. P. Surendran, N. Santha, P. Mohanan and M. T. Sebastian. Eur. Phys. J. B41 (2004) 301.

[13] H. Maekawa, S. Kato, K. Kawamura and T. Yokokawa, Am. Meneralogist. 82 (1997) 1125.

[14] V. Šepelák, S. Indris, I. Bergmann, A. Feldhoff, K. D. Becker, and P. Heitjans, Solid. State. Ionics. 177 (2006) 2487.

[15] S. Takahashi, A. Kan and H. Ogawa, J. Eur. Ceram. Soc. 37 (2017) 1001.

[16] H. M. Rietveld, J. Appl. Crystallor. 2 (1969) 65.

[17] F. Izumi, and K. Momma, Solid State Phenom. 130 (2007) 15.

[18] B. W. Hakki, P. D. Coleman, and I. R. E. Trans, Microwave Theory Tech. 8 (1960) 402.

[19] Y. Kobayashi and M. Katoh, IEEE Trans. Microwave Theory Tech. 33 (1985) 586.

[20] S. M. Hosseini. Phys. Status Solid. B. 245 (2008) 2800.

[21] O. Medenbach, T. Siritanon, M. A. Subramanian, R. D. Shannon, R. X. Fischer and G. R. Rossman, Mater. Res. Bull. 48 (2013) 2240.

[22] R. L. Millard, R. C. Peterson and B. K. Hunter, Amer. Mineral. 77 (1992) 44.

[23] E. S. Blaakmeer, F. Rosciano and E. R. H. Eck, J. Phys. Chem. 119 (2015) 7565.

[24] S. Takahashi, A. Kan, and H. Ogawa, J. Eur. Ceram. Soc. 37 (2017) 1001.

[25] R. D. Shannon, Acta Crystaalogr. 32 (1976) 751.

[26] P. Nadia, D. T. Catherine, M. Valérie, B. Michel, and M. Dominique, J. Phys. Chem. B 111 (2007) 12707.

[27] R. D. Shannon, J. Appl. Phys. 73 (1993) 348.

[28] C. W. Zheng, S. Y. Wu, X. M. Chen and K. X. Song, J. Am. Ceram. Soc. 90 (2007) 1483.

Caption

Fig.1. XRPD profiles of (a) calcined-MAO*n* and (b) -ZAO*n* powders with different duration of ball-milling.

Fig. 2. Particle size distributions of (a) calcined-MAO*n* and (b) -ZAO*n* powders with different duration of ball-milling.

Fig. 3. ^{27}Al NMR spectra of (a) calcined-MAO*n* and (b) -ZAO*n* powders with different duration of ball-milling.

Fig.4. FE-SEM images of (a) MA0h, (b) MA24h, (c) ZA0h and (d) ZA24h ceramics fired at 1600 °C for 5 h.

Fig.5. XRPD profiles of $Mg_{1-x}Zn_xAl_2O_4$ ceramics fired at 1600 °C for 5 h over the 2θ ranges of (a) 10–70° and (b) 34–40°.

Fig.6. ^{27}Al NMR spectra of (a) calcined-$Mg_{1-x}Zn_xAl_2O_4$ powders and (b) $Mg_{1-x}Zn_xAl_2O_4$ ceramics fired at 1600 °C for 5 h.

Fig.7. Composition dependence of relative density and dielectric constant (ε_r) of $Mg_{1-x}Zn_xAl_2O_4$ ceramics fired at 1600 °C for 5 h.

Fig.8. Effects of Zn substitution for Mg on (a) $Q \cdot f$ and (b) TCf values of $Mg_{1-x}Zn_xAl_2O_4$ ceramics fired at 1600 °C for 5 h.

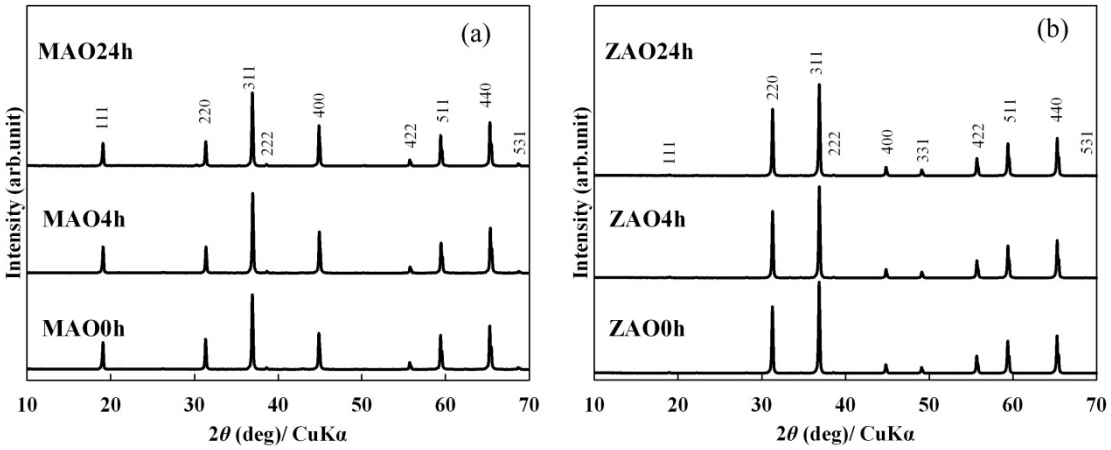

Fig.1. XRPD profiles of (a) calcined-MAO*n* and (b) -ZAO*n* powders with different duration of ball-milling.

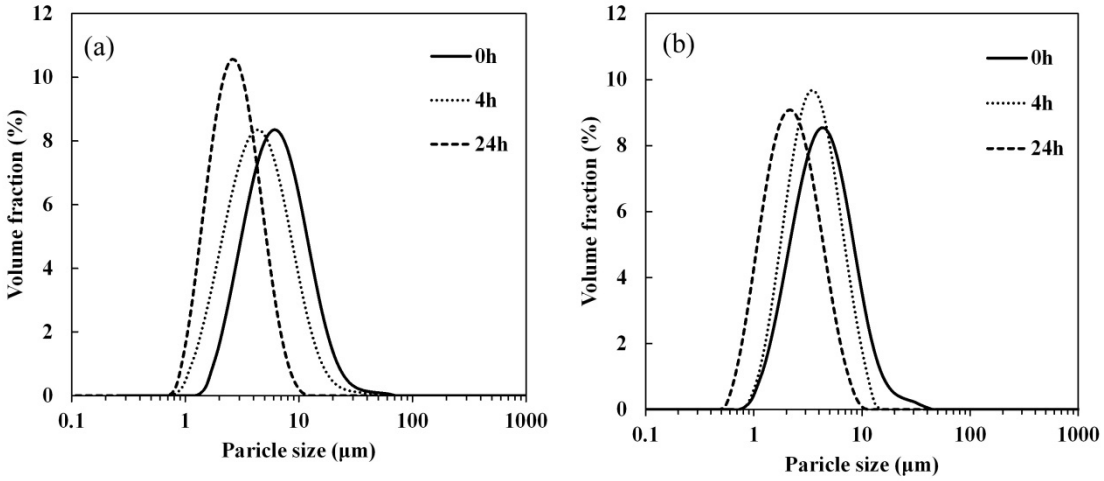

Fig. 2. Particle size distributions of (a) calcined-MAO*n* and (b) -ZAO*n* powders with different duration of ball-milling.

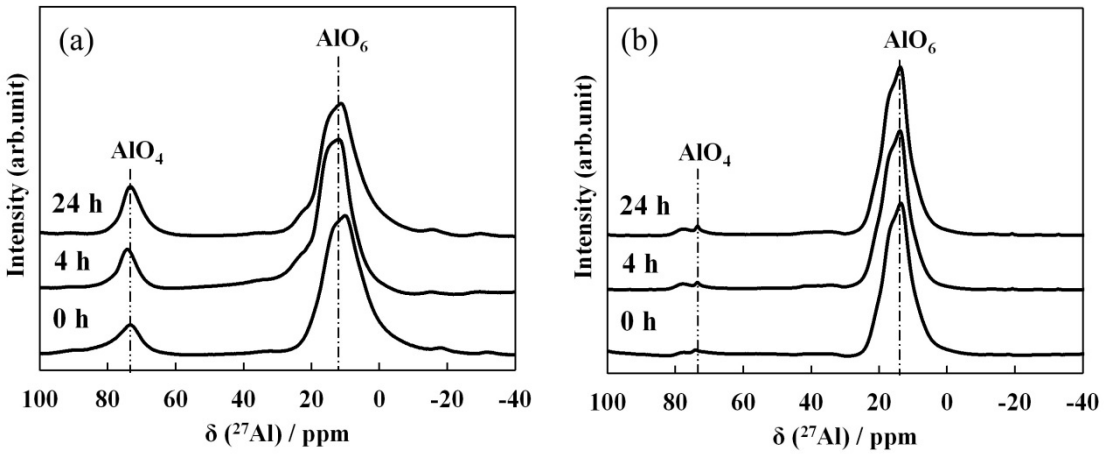

Fig. 3. ^{27}Al NMR spectra of (a) calcined-MAO*n* and (b) -ZAO*n* powders with different duration of ball-milling.

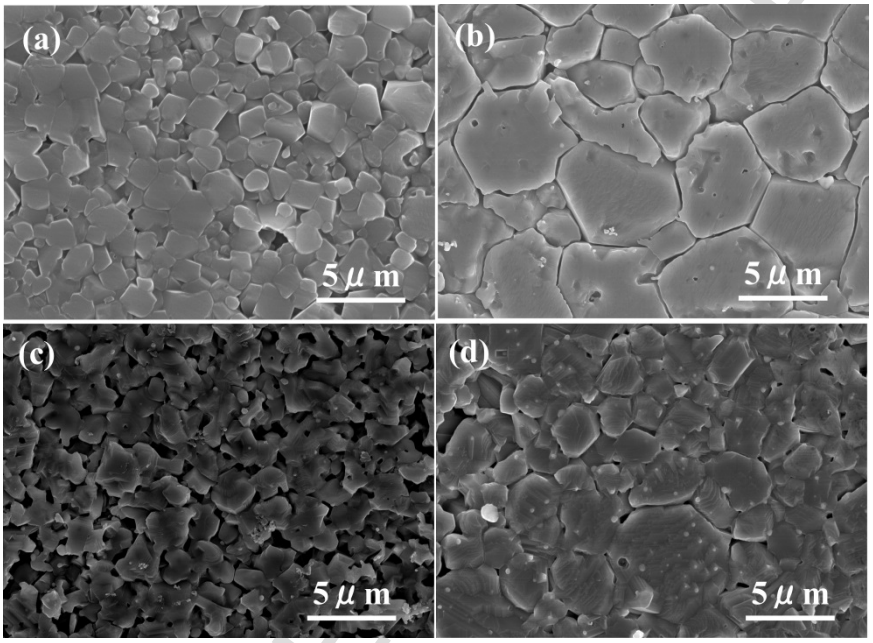

Fig.4. FE-SEM images of (a) MA0h, (b) MA24h, (c) ZA0h and (d) ZA24h ceramics fired at 1600 °C for 5 h.

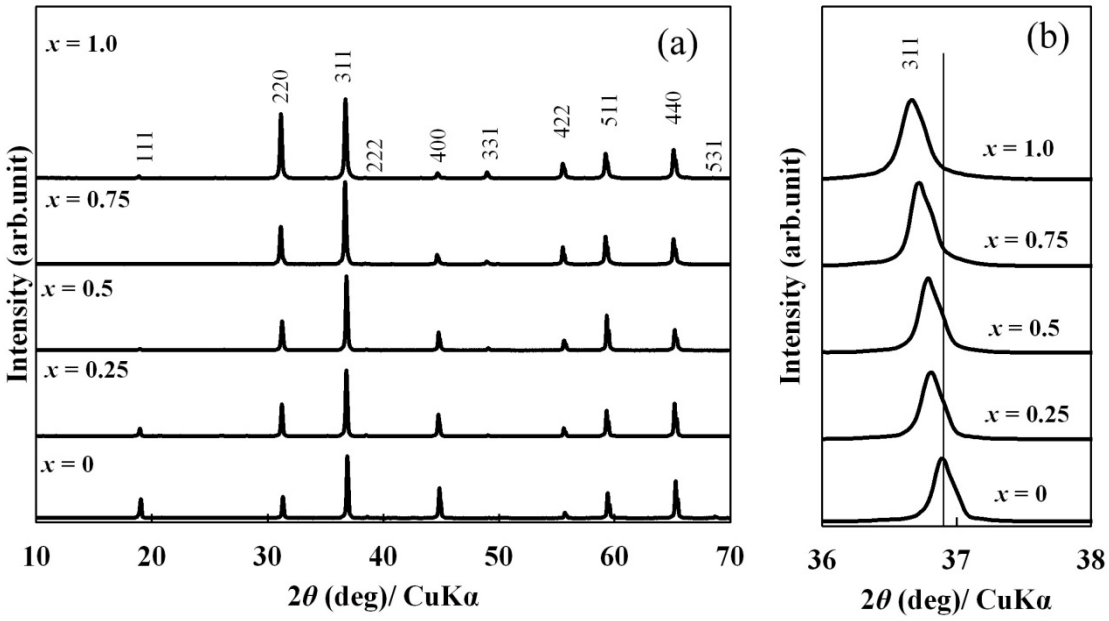

Fig.5. XRPD profiles of $Mg_{1-x}Zn_xAl_2O_4$ ceramics fired at 1600 °C for 5 h over the 2θ ranges of (a) 10–70° and (b) 34–40°.

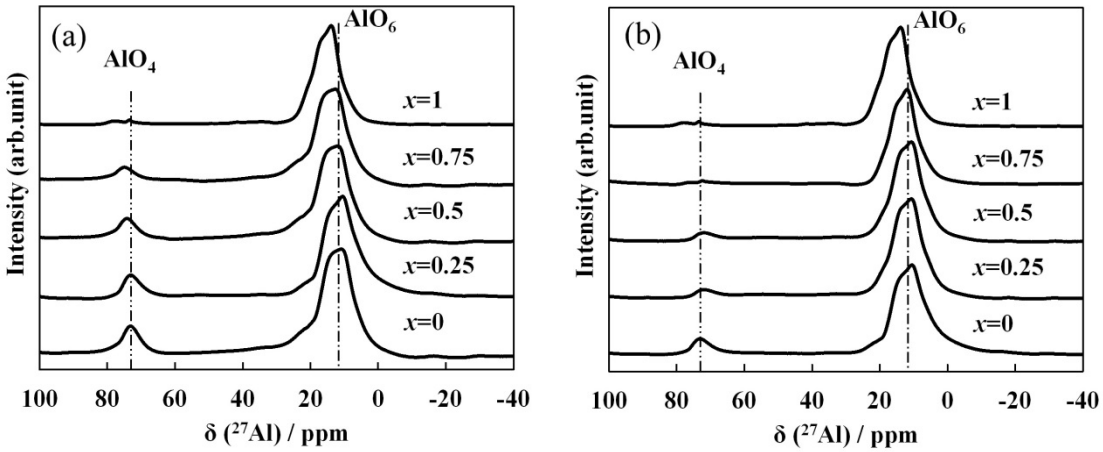

Fig.6. ^{27}Al NMR spectra of (a) calcined-$Mg_{1-x}Zn_xAl_2O_4$ powders and (b) $Mg_{1-x}Zn_xAl_2O_4$ ceramics fired at 1600 °C for 5 h.

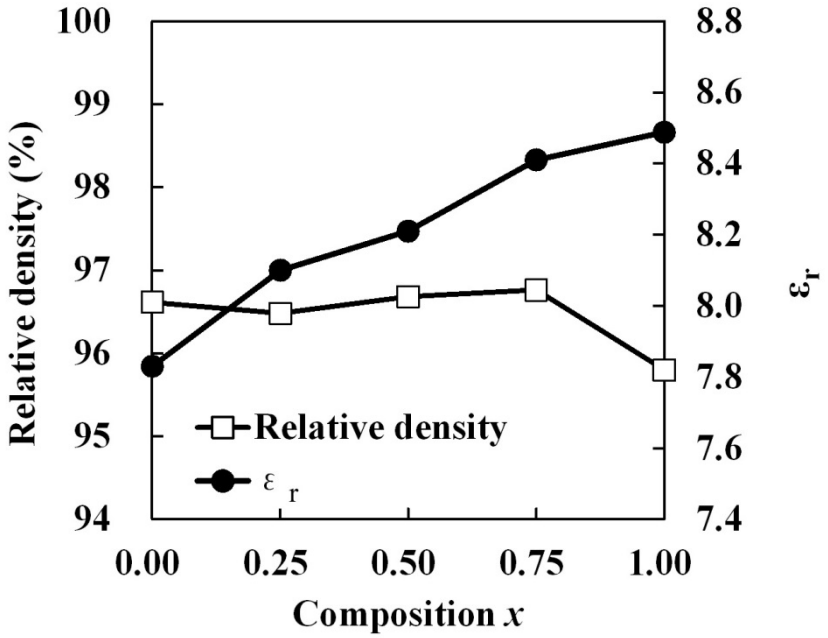

Fig.7. Composition dependence of relative density and dielectric constant (ε_r) of $Mg_{1-x}Zn_xAl_2O_4$ ceramics fired at 1600 °C for 5 h.

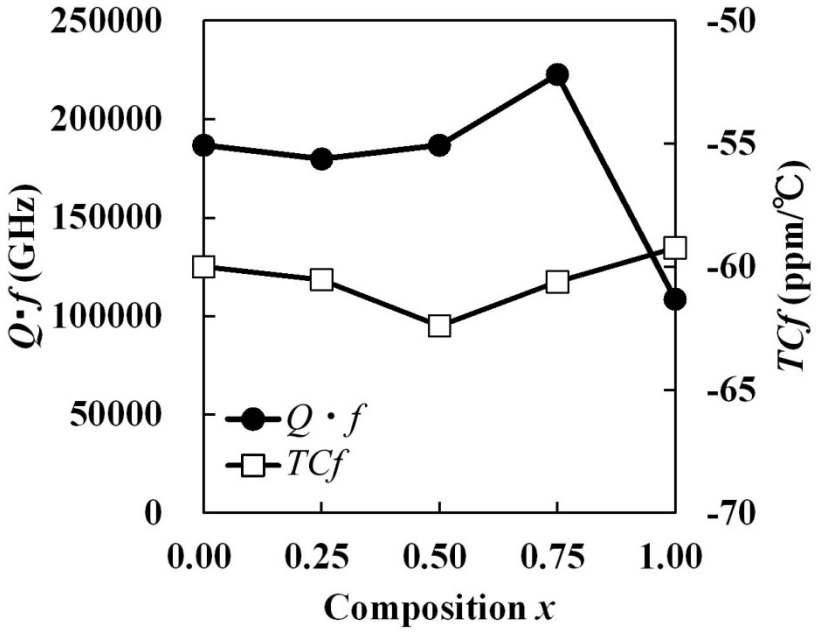

Fig.8. Effects of Zn substitution for Mg on (a) *Q·f* and (b) *TCf* values of $Mg_{1-x}Zn_xAl_2O_4$ ceramics fired at 1600 °C for 5 h.

Highlights

- The preferential occupation of Al^{3+} cation in tetrahedral site was obtained for $MgAl_2O_4$.

- The ball-milling of the calcined-$MgAl_2O_4$ powders enhanced the $Q \cdot f$ value of the ceramics.

- The Zn substitution for Mg of the $Mg_{1-x}Zn_xAl_2O_4$ ceramics led to the enhancement of $Q \cdot f$ value of the ceramics.

Table 1. Median sizes of calcined-MAO*n* and ZAO*n* powders, FWHM values of (311) plane and degree of inversion (λ_C and λ_F) of calcined-MAO*n* and ZAO*n* powders and MA*n* and ZA*n* ceramics, and degree of redistribution of Al^{3+} cation in octahedral site during firing (λ_0)

Table 2. Crystal structure parameters of MA*n* and ZA*n* ceramics fired at 1600 °C for 5 h using the calcined powders with different duration of ball-milling.

Table 3. Relative density and dielectric properties (ε_r and $Q \cdot f$) of MA*n* and ZA*n* ceramics fired at 1600 °C for 5 h using the calcined powders with different duration of ball-milling.

Table 4. Crystal structure parameters of $Mg_{1-x}Zn_xAl_2O_4$ ceramics.

Table 5. FWHM value ($FWHM_C$ and $FWHM_F$) and degree of inversion (λ_C and λ_F) of $Mg_{1-x}Zn_xAl_2O_4$ powders and ceramics, and degree of redistribution of Al^{3+} cation in octahedral site during firing (λ_0).

Table 1. Median sizes of calcined-MAO*n* and ZAO*n* powders, FWHM values of (311) plane and degree of inversion (λ_C and λ_F) of calcined-MAO*n* and ZAO*n* powders and MA*n* and ZA*n* ceramics, and degree of redistribution of Al^{3+} cation in octahedral site during firing (λ_0)

Composition	Duration of ball-milling (h)	Median size of calcined-powder (μm)	$FWHM_C$ (°)	$FWHM_F$ (°)	λ_C	λ_F	λ_0
$MgAl_2O_4$	0	4.39	0.254	0.157	0.33	0.27	0.06
	4	4.02	0.257	0.156	0.35	0.28	0.07
	24	2.49	0.265	0.138	0.42	0.29	0.13
$ZnAl_2O_4$	0	4.00	0.255	0.156	0.04	0.03	0.01
	4	3.25	0.258	0.155	0.06	0.03	0.03
	24	2.04	0.264	0.152	0.07	0.03	0.04

Table 2. Crystal structure parameters of MA*n* and ZA*n* ceramics fired at 1600 °C for 5 h using the calcined powders with different duration of ball-milling.

Composition	Duration of ball-milling (h)	Lattice parameter *a* (Å)	Theoretical density (g/cm^3)	*M*-O bond length (Å)	
				MO_4	MO_6
$MgAl_2O_4$	0	8.0716(8)	3.58(1)	1.903(7)	1.935(1)
	4	8.0709(2)	3.58(2)	1.903(1)	1.934(4)
	24	8.0677(9)	3.58(6)	1.901(3)	1.933(9)
$ZnAl_2O_4$	0	8.0807(7)	4.62(3)	1.948(1)	1.921(8)
	4	8.0802(4)	4.62(4)	1.948(3)	1.920(5)
	24	8.0793(4)	4.62(6)	1.947(9)	1.911(2)

Table 3. Relative density and dielectric properties (ε_r and $Q \cdot f$) of MA*n* and ZA*n* ceramics fired at 1600 °C for 5 h using the calcined powders with different duration of ball-milling.

Composition	Duration of ball-milling (h)	Relative density (%)	ε_r	$Q \cdot f$ GHz)
$MgAl_2O_4$	0	94.8	7.8	85,100
	4	95.2	7.8	87,300
	24	96.6	7.9	197,200
$ZnAl_2O_4$	0	95.0	8.5	93,300
	4	95.4	8.5	94,400
	24	95.6	8.5	108,500

Table 4. Crystal structure parameters of $Mg_{1-x}Zn_xAl_2O_4$ ceramics.

Sample	Composition	Lattice parameter *a*	Theoretical density	*M*-O bond length (Å)	
	x	(Å)	(g/cm^3)	MO_4	MO_6
$Mg_{1-x}Zn_xAl_2O_4$	0	8.0677(9)	3.58(6)	1.901(3)	1.933(9)
	0.25	8.0702(3)	3.81(4)	1.922(9)	1.930(2)
	0.5	8.0737(2)	4.13(8)	1.932(2)	1.925(5)
	0.75	8.0767(5)	4.33(2)	1.939(8)	1.919(6)
	1	8.0793(4)	4.62(6)	1.947(9)	1.911(2)

Table 5. FWHM value ($FWHM_C$ and $FWHM_F$) and degree of inversion (λ_C and λ_F) of $Mg_{1-x}Zn_xAl_2O_4$ powders and ceramics, and degree of redistribution of Al^{3+} cation in octahedral site during firing (λ_0).

Sample	Composition *x*	$FWHM_C$ (°)	$FWHM_F$ (°)	λ_C	λ_F	λ_0
$Mg_{1-x}Zn_xAl_2O_4$	0	0.257	0.138	0.42	0.29	0.13
	0.25	0.258	0.136	0.35	0.22	0.13
	0.5	0.260	0.136	0.29	0.14	0.15
	0.75	0.260	0.132	0.21	0.04	0.17
	1	0.263	0.152	0.07	0.03	0.04